

# From single neuron dynamics to emergent spatio-temporal states in networks

Supervisor: Dr. Magnus Richardson  
*Warwick Systems Biology Centre  
University of Warwick,  
Coventry CV4 7AL, United Kingdom*

Author: Ramón Heberto Martínez Mayorquin\*  
*Centre for Complexity Science  
University of Warwick,  
Coventry CV4 7AL, United Kingdom*  
(Erasmus Mundus M1 Written Report  
Complex Systems Science)  
(Dated: June 24, 2013)

Integrate and Fire models are used as semi-detail models of the biophysics of the firing rate. Firing Rate Models on the other hand disregard the biology and try to model the dynamics of the firing rate in another time scale. In this work we study the dynamics of the firing rate in Spike Models and study how the parameters of Firing Rate Models under can be related to the parameters of Spiking Rate Models. Finally we use this relation to build a Spatial Network model that takes into account this link.

## I. INTRODUCTION

On the most important problems for creating a general theory of how the brain works is to understand how the different scales of the brain processes interact between themselves and how the bottom processes levels give rise to the upper ones. In this work we try to advance a small step in this direction by exploring the relations between spiking models (Particularly the Exponential Integrate and Fire model) and network models.

This work is structured in the following way. First we review the general background and Biophysics required to construct a model of membrane voltage dynamics. The concept of the firing rate is introduced afterwards and so are Spiking Models. The dynamics of the firing rate induced by Spiking Models are presented in some detail also. We then proceed to the study of spatial networks via a Firing Rate Model. One of the core arguments developed in this work is that the Exponential and Integrate Spiking Model in particular can be related in a direct fashion to a Firing Rate Model through their asymptotic behaviour providing a link between two different scales of brain processing. Finally we summarize with a discussion about the results and present plans of future work.

## II. GENERAL BACKGROUND

### A. Biophysics of Neural Excitability

Perhaps the most amazing and unique ability of neurons is to communicate through propagation of electrical

signals. In this section we briefly review the fundamentals of how this signals are produced and maintained.

The usual quantity used to characterise the electrical behaviour of the neuron is the difference of electrical potential between the interior and the exterior of the cell, that particular potential is called **Membrane Voltage** and is denoted by  $V_m$ . It turns out that under normal circumstances the value of this quantity is usually in the range of  $-60$  to  $-70$  mV. This difference arises from a separation of charges across the cell membrane. That is, in steady state there is an excess of negative charge inside and of positive charge outside [1].

The membrane of the cell is a lipid bilayer which due to his biophysical nature block the pass of ions and therefore works as an insulator. On the other hand the cytoplasm and the extracellular medium are conductive media. We have an insulator between two conductive media which from the point of view of electrical circuit theory is a capacitor and the next relation holds:  $Q = CV_m$ .

A prominent feature of the cell membrane is the presence of membrane spanning proteins called **Ion Channels** [2]. These proteins allow the ions to move from one side of the membrane to the other and therefore shape the electrical profile of the neuron. In order to account for the dynamics of a particular species of ions we have to take into account two factors: diffusion due to gradient of concentrations and electrical forces due to the fact that ions are charged particles.

#### *Diffusion in an ion channel*

Next we aim to construct a model for the flux of ions. As we mentioned before we have two contributions: first and electrical term which is related to ions drifting due to their electrical nature that takes the following form  $J_{drift} = vN$  where  $v$  is called the drift term and  $N$  stands

---

\*h.mayorquin@gmail.com

for the concentration of the ion. Furthermore the drift term can be written  $v = \mu \text{Force} = -\mu z q \frac{\partial V}{\partial x}$  where  $\mu$  is the mobility,  $q$  is the charge of the proton and  $z$  is the valence. Note that we have written the force as a gradient of the potential here.

On the other hand the term for the diffusion can be derived from Fick's first law:  $J_{diff} = -D \frac{\partial N}{\partial x}$ . Where the diffusion constant  $D$  can be written in terms of the mobility and the Boltzman's constant  $D = \mu k_B T$ . Here  $T$  stands for absolute temperature.

Now that we have the two components of the flux we can express the totality of it as:

$$J = J_{drift} + J_{diff} \quad (1)$$

$$J = vN - D \frac{\partial N}{\partial x} \quad (2)$$

Which then we rewrite as:

$$J = -\mu k_B T \left( N \frac{z}{V_T} \frac{\partial V}{\partial x} + \frac{\partial}{\partial x} \right) \quad (3)$$

Where  $V_T = k_B T$  is the thermal energy.

#### Nerst Equation

From 3 we can get the membrane potential at which the flux stops (the flux is zero) for that particular ion, this provide us with the famous **Nerst Equation**:

$$E = \frac{V_T}{z} \log \left( \frac{N^e}{N^i} \right) \quad (4)$$

Where  $N^e$  and  $N^i$  are the outside concentration and the inside concentration respectively.

#### Goldman Current

From 3 we can also calculate the current that flows when the membrane potential differs from the 4.

$$I = \frac{Pz^2q}{V_T} V_m \left( \frac{N^e - N^i e^{\frac{zV}{V_T}}}{1 - e^{\frac{zV}{V_T}}} \right)$$

Where we have introduce the permeability  $P = \frac{D\rho\sigma}{a}$ . We then can linearise the expression to get an ohm-like relation:

$$I = g(V - E) + O((V - E)^2) \quad (5)$$

Where we can identify a conductance per unit area  $g$ :

$$g = \frac{Pz^2q}{V_T} N^e N^i \left( \frac{\log(N^e/N^i)}{N^e - N^i} \right)$$

#### The Voltage Equation for a Passive Membrane

So we have a capacitive current for the membrane  $C \frac{dV}{dt}$  and another current due to the ion channels 5. Using Kirchhoff's law we can write:

$$C \frac{dV}{dt} + g(V - E) = 0$$

Rearranging we have our voltage equation for a passive membrane:

$$\tau \frac{dV}{dt} = E_L - V; \quad (6)$$

Where  $\tau = C/g$  is the time constant of the circuit.

### B. The Action Potential

Neurons are able to carry signals over long distances because of their ability to generate **action potentials** a regenerative electrical signal whose amplitude does not notoriously decrease as it travels along the axon [1].

A particular characteristic of actions potentials are threshold voltages. If we perturb the voltage from its usual resting state two things can happen: either the perturbation are not strong enough and the the current will do a brief detour from equilibrium just to return after it -yellow trajectories in figure 1- or if the perturbation is strong enough it will push the neuron above the threshold -orange trajectory in figure 1- and a trajectory like the one described in the figure will ensue.

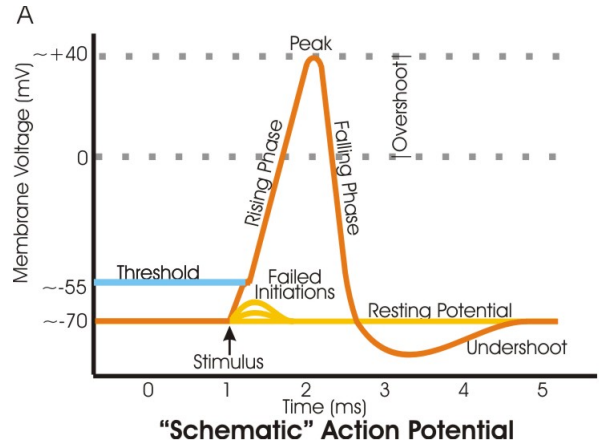


FIG. 1. Schematic of an action potential. Both kind of perturbations and the resulting trajectories are illustrated in this schematic. Image modified from Wikipedia Commons

### C. Firing Rate

Action potentials are highly stereotyped events. In this work we are interested in counting the number of action potentials also called spikes per unit of time. That is, we are interested in studying the dynamics of what is called the **firing rate**.

In the first half of the last century Adrian established that the average firing rate was the way in which the nervous system coded for intensity of stimulus muscle [3]. He found a relationship between the firing rate and the weight applied in the muscle. The problem of how the brain uses the rate to code for certain task and dynamics and models and calculations of how firing rate behaves remain of widespread interest in the scientific community even today [4].

A brief survey in the relevant literature will allow us to see that there is more than one reasonable way of assigning meaning to what we call the firing rate (See [5],[4] or [6] for example). There is at least three definitions of rate in the literature. The most basic one is **Rate as a Spike Count** which appeared as early as in the work of Adrian. The idea is just to count the number spikes  $N_{sp}$  in a given time interval and then divide by the length of the time interval:

$$r = \frac{N_{sp}}{T} \quad (7)$$

A characteristic of this quantity is that the broad coarse average washes away the time evolution of the quantity. However our objective is to measure the effects of time dependent perturbations, therefore we need to find a way to include instant variations in the firing rate. In other words we need a time dependent firing rate.

One of the ways to include time dependence is the definition of rate as **Population Activity**. This definition considers a perfectly homogeneous population of  $N$  neurons and then proceeds to count the number of neurons  $n(t, t + \Delta t)$  which are active in an time interval of size  $\Delta t$ . The outcome averaged over the whole population is defined as the instantaneous firing rate so we can write:

$$r(t) = \frac{1}{\Delta t} \frac{n(t, t + \Delta t)}{N} \quad (8)$$

#### *Diffusion Approximation*

Neurons receive in average 6000 [7] inputs from other neurons. Trying to model such a myriad of effects deterministically will make our model too complex for analysis. An usual approach to avoid that shortcoming is to model the cumulative effect of this background as an stochastic process. If we assume that each input is an independent Poisson Process with a small effect then we can build a Fokker Planck Equation for the probability

distribution of the voltage and end up with an stochastic differential equation for the voltage of the following form [5]

$$\tau_m \frac{dV}{dt} = E_0 - V(t) + \sigma_V \sqrt{2\tau_m} \xi(t) \quad (9)$$

Where  $\xi$  is Gaussian White Noise and the following properties hold for it: First is average is given by  $\langle \xi(t) \rangle = 0$  while the next property holds for the autocorrelation  $\langle \xi(t) \xi(t') \rangle = \delta(t - t')$ . The equation above is an stochastic differential equation and is an example of an Ornstein-Uhlenbeck process.

### III. INTEGRATE AND FIRE MODELS

In this work we are interested in the dynamics of the firing rate. In consequence we need a model that is capable of generate action potentials. The classical work in action potential generation by Hodgking and Huxley [8] resorts to voltage dependent conductivities for the ion channels as the cause of spike's dynamics.

Hodgking and Huxley models provide the time at which the action potential occur but also provide the whole trajectory in all its detail. Nevertheless in this work we are mainly interested in the time at which these events happen and we would like to make a simplification that disregards full action potential's dynamics for the sake of computational efficiency. One plausible avenue of simplification comes from Integrate and Fire Models. Integrate and Fire models were introduced by Lapique hundred years ago [9] and are still widely used today in the scientific community to model a variety of effects [10].

Integrate and Fire models basic idea is illustrated in the figure 2. We define two voltage points  $V_{re}$  and  $V_{th}$  that will control the time of spike events in our system in the following way: we start our voltage trajectory at  $V_{re}$  and evolve the system under his own dynamics -given by whatever model we chose for this aim- and when voltage surpasses  $V_{th}$  we immediately reset voltage value to  $V_{re}$ , the cycle repeats itself and the timing is register.

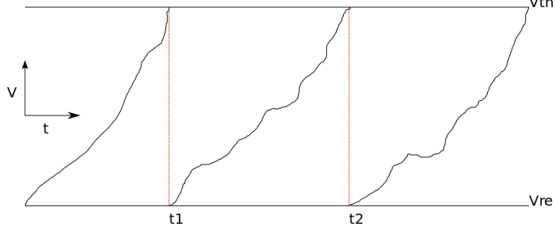


FIG. 2. Schematics of Integrate and Fire Models illustrating the main features of this model. We evolve the voltage accordingly to a particular model that we chose. When the value of a particular voltage trajectory surpasses  $V_{th}$  we reset the value to  $V_{re}$  register the time as an occurrence of an action potential and repeat the process again.

Now we proceed to present the particular dynamics that we are going to use in this work with an Integrate and Fire scheme.

#### Leaky Integrate and Fire (LIF)

The Leaky Integrate and Fire model (LIF) is just eq 6 in the context of Integrate and Fire Models. Taking this into account the dynamics are given by:

$$\tau \frac{dV}{dt} = E - V \quad (10)$$

It follows straightforward from the equation that we are going to have spikes in this models if and only if  $E > V_{th}$ .

#### Exponential Integrate and Fire (EIF)

Another popular integrate and fire model is the exponential integrate and fire (EIF) model [11]. It captures the initial dynamics of the opening of the spike generating sodium channels responsible for action potentials in other models. This initial effect is model by an exponential term  $\psi(V) = \Delta_T e^{\frac{V-V_T}{\Delta_T}}$ . Therefore we can write:

$$\tau \frac{dV}{dt} = E + \Psi(V) - V \quad (11)$$

A similar reasoning that the one above can show us that this model also has a threshold and it not going to fire when  $E$  is below that particular value.

#### A. Simulations

We used a Forward Euler Method to simulate the SDEs. First for the (LIF) where we updated our pro-

cess a time  $dt$  with the usual formula:

$$V(t + dt) = V(t) + \frac{dt}{\tau} (E - V(t)) + \sigma \sqrt{2 \frac{dt}{\tau}} N(0, 1) \quad (12)$$

Where  $N(0, 1)$  is a normal distribution with mean 0 and 1 as variance as usual. On the other hand for the (EIF) the scheme is given by:

$$V(t + dt) = V(t) + \frac{dt}{\tau} (E - V(t) + \psi(V(t))) + \sigma \sqrt{2 \frac{dt}{\tau}} N(0, 1) \quad (13)$$

Where  $\psi(V) = \Delta_T e^{\frac{V-V_T}{\Delta_T}}$

Furthermore we compare the quantities obtained by the simulations to those obtained by a methodology described by [12].

#### LIF - Steady State

First we simulated how the steady state firing rate was affected by changes in the parameter  $E$ . We show the outcomes of the simulations in figures 3 and 4.

In figure 3 we have the simulation corresponding to the low noise case (small  $\sigma$ ). We can appreciate a threshold-like behaviour at  $E = -53$ . That is, we don't have significant firing until  $E$  is above that value.

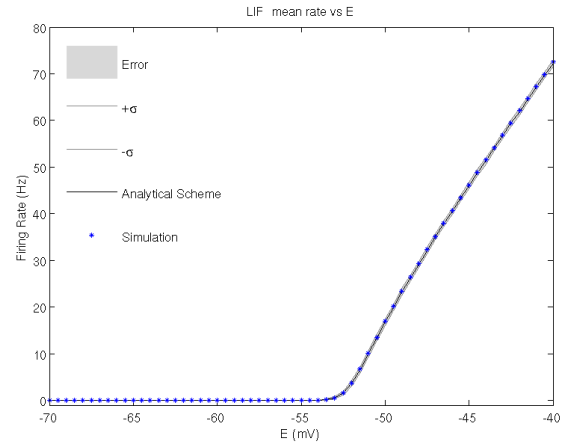


FIG. 3. Steady state  $r$  dependence on  $E$  for an LIF model. Here  $\sigma = 1$ , the rest of the parameters are  $\tau = 20$  ms,  $V_{th} = -50$  mV,  $V_{re} = -60$  mV. Here we used a simulation step size of  $dt = 0.01$  ms. Note how we have threshold behaviour. For some values of the  $E$  there is almost no fire until a critical value is reached.

On the other hand in figure 4 we illustrated the case with considerable noise (relatively big  $\sigma$ ). The most fundamental departure from the low noise case the fact

that we have firing below the expected level. This sub-threshold firing behavior appears marking a difference with the low noise case. The phenomenon appears because when we are close to the threshold value the noise can put us above it and therefore we can have firing even if the deterministic dynamics of the system don't allow it.

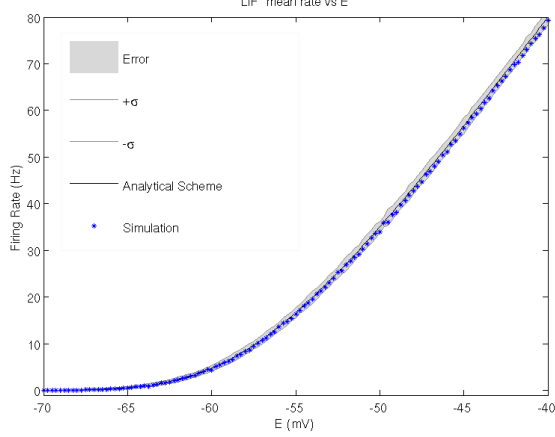


FIG. 4. Steady state  $r$  dependence on  $E$  for an LIF model. Here  $\sigma = 5$  mV, the rest of the parameters are  $\tau = 20$  ms,  $V_{th} = -50$  mV,  $V_{re} = -60$  mV. We used a simulation step size of  $dt = 0.01$  ms. A notable feature worth to emphasize is sub-threshold firing for the high noise case. That is if we compare this case with the one in figure 3 we can immediately tell that we have significant firing rate for values below the threshold.

### EIF

Simulation of the exponential integrate and fire provided us with similar outcomes. Here again we have two regimes: the low noise one and the high noise one. We illustrate the results in figures 5 and 6.

First in figure 5 we appreciate the phenomenon of a threshold appearing around  $-57$  mV as in the previous case.

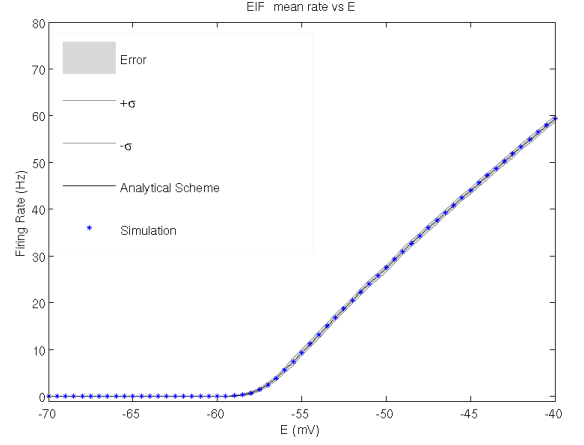


FIG. 5. Steady state  $r$  dependence on  $E$  for an EIF model. Here  $\sigma = 2$  mV. The rest of the parameters are  $\tau = 20$  ms,  $V_{th} = -50$  mV,  $V_{re} = -60$  mV,  $\Delta_T = 3$  mV and  $V_T = -53$  mV. We used a simulation step size of  $dt = 0.01$  ms.

In figure 6 the outcomes of the high noise simulations for the EIF are presented. Again the most conspicuous fact to note is the sub-threshold firing behaviour.

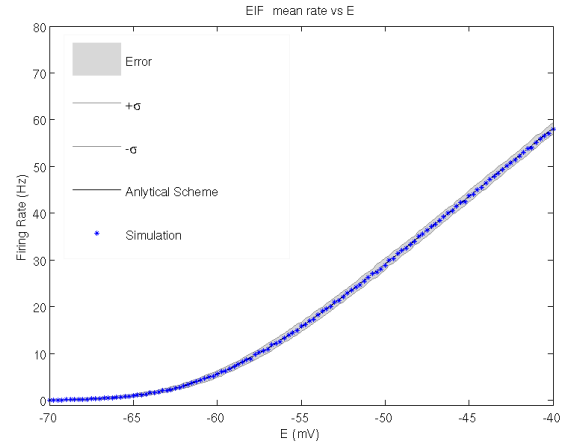


FIG. 6. Steady state  $r$  dependence on  $E$  for an EIF model. Here  $\sigma = 2$  mV for the one on the left and  $\sigma = 6$  mV for the one on the right. The rest of the parameters are  $\tau = 20$  ms,  $V_{th} = -50$  mV,  $V_{re} = -60$  mV,  $\Delta_T = 3$  mV and  $V_T = -53$  mV. We used a simulation step size of  $dt = 0.01$  ms. Again it is worthwhile to emphasize the fact that sub-threshold firing appears.

### Perturbation

We are interested in what is our system response to a time dependent perturbation so we propose a simple one to start. We subject our neuron to a temporal perturbation in  $E$  of the following form:

$$E(t) = E_0 + E_1 \cos(\omega t) \quad (14)$$

This implies variations in all states variables including the rate [12] :

$$r(t) = r_0 + r_E \cos(\omega t + \rho_E) \quad (15)$$

In the following sections we present at detail how the systems deviates from equilibrium under a perturbation of the kind presented in equation 14. To obtain the results we simulated the system for each one of the frequencies and then fitted the outcomes to the appropriated trigonometric curve. The results are contrast again the results obtained from another methodology from the literature [12].

### LIF - Modulated

Finally we present the simulation of the time dependent modulated system. We illustrate our results in figures 7 and 8.

In the figure 7 we illustrate how the properties of the rate perturbation vary as a function of the frequency for perturbations under low noise (small  $\sigma$ ). We found that for low frequency the perturbation in the rate is stable and doesn't change, so in the low frequency domain our rate perturbation is constant. A notorious feature of the graph is the resonance for frequencies close to the  $r_0$ . For the high frequency domain we observe a steady decline.

For the phase as a function of the frequency we found that the phase behaviour changes his regime at the firing rate and after it heads towards an asymptote of  $-45$  degrees.

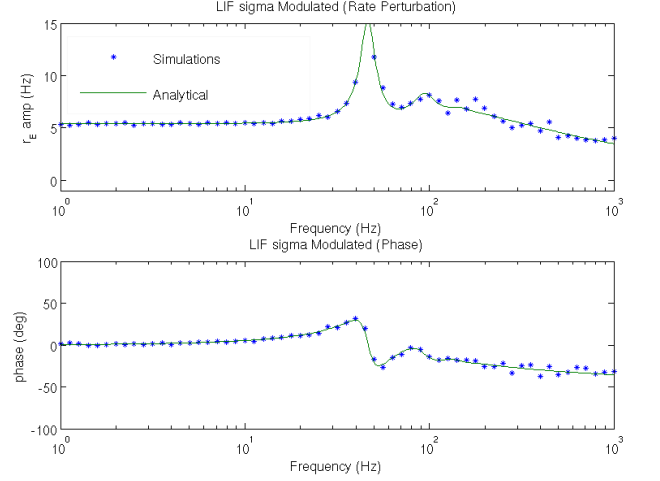


FIG. 7. LIF modulated for low noise ( $\sigma = 2$ ). For this simulation we used the parameters  $V_{th}$  mV,  $V_{re}$  mV and  $\tau = 20$  ms. In the upper image we have the size of the perturbation on the rate as function of the frequency. In the image below we have the variation of the phase of the perturbation as a function of the frequency.

On the figure 8 we illustrate how modulated perturbations affect the rate in the high noise regime (relatively big  $\sigma$ ). In this case we found a similar behaviour to the one with low noise except for the disappearance of the resonance. So in this case the noise is capable of destroying the resonance, that is, the synchrony of the system and the perturbation.

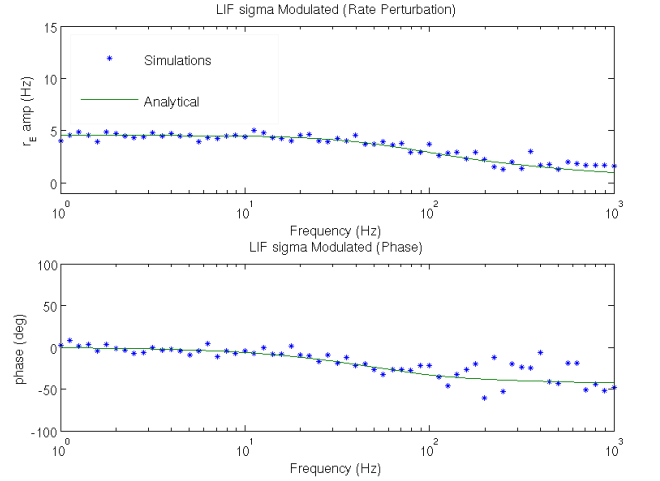


FIG. 8. LIF modulated for high noise ( $\sigma = 6$ ) For this simulation we used the parameters  $V_{th}$  mV,  $V_{re}$  mV and  $\tau = 20$  ms.

### EIF - Modulated

And then we have the modulation for the EIF modulated case. We illustrate our results in figures 9 and

10.

In figure 9 we have the simulation for the low noise (small  $\sigma$ ) case. In the picture above we plot the size of the resulting perturbation as a function of the frequency while in the picture below the phase as a function of the frequency is presented. The shape of the resulting curve is remarkably similar with the one of the LIF model, we found a low frequency regime with constant perturbation size, a middle one with prominent resonance and a higher frequency domain with decaying perturbation. The most high profile difference between the behaviours is perhaps that the EIF decays faster.

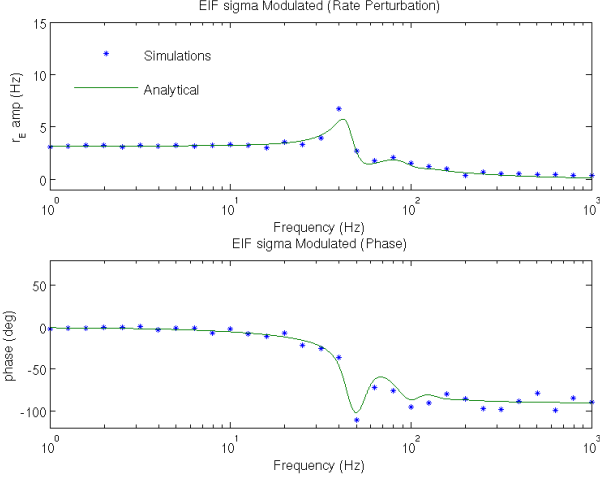


FIG. 9. modulated for low noise ( $\sigma = 2$ ). For this simulation we used the parameters  $V_{th}$  mV,  $V_{re}$  mV and  $\tau = 20$  ms.

In figure 9 we have the simulation for the high noise regime (relatively big  $\sigma$ ). Again this picture is remarkably similar in a qualitatively way to the LIF case. Two notorious differences however are first that the EIF decays faster and that the phase goes below his asymptote value for some frequencies.

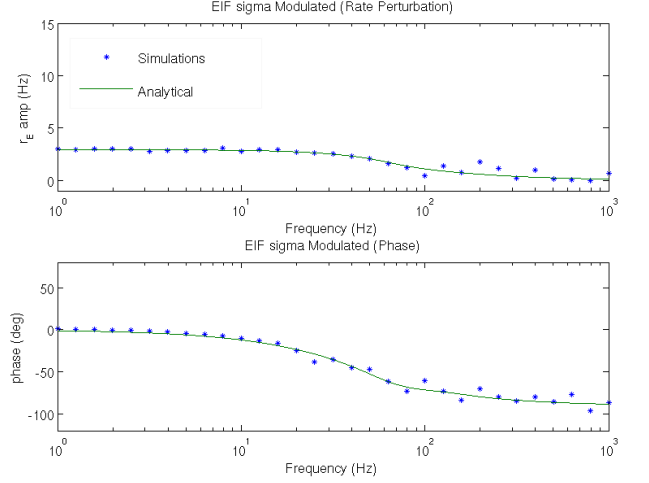


FIG. 10. EIF modulated for high noise ( $\sigma = 6$ ) For this simulation we used the parameters  $V_{th}$  mV,  $V_{re}$  mV and  $\tau = 20$  ms.

## IV. NETWORK MODELS

### A. Rate Model and Asymptotic Fixing

Firing rate models are models of neural networks where the dynamics of the voltage are ignored and instead we focus on the sole dynamics of the firing rate [6]. In general Spiking models involve a time scale small enough to capture the effects responsible for taking a particular voltage trajectory over the threshold, that is, the dynamics that lead the model to an action potential. Firing rate models suppress that temporal scale and therefore are simpler in that particular way, in other words, they belong to a different time scale.

$$\tau \frac{dr}{dt} = \Phi(E) - r \quad (16)$$

Here  $\Phi(E)$  is equal to the steady state firing rate  $r_0$  for a particular value of  $E$ .  $\tau$  on the other hand is a measure of how fast  $r$  averages to  $r_0$  following a change in  $E$ .

If we consider a small modulation in  $E$  in the following way  $E = E_0 + E_1 e^{i\omega t}$  we can expand  $\Phi$  in  $E$  in its Taylor's series and disregard everything but the linear term:

$$i\omega\tau r_1 e^{i\omega t} = \Phi(E_0) + \frac{d\Phi}{dE} E_1 e^{i\omega t} - r_0 - r_1 e^{i\omega t} \quad (17)$$

Moreover by definition  $\Phi(E_0) = r_0$ . Using this expression we can rearrange the terms in the following way:

$$r_1(1 + i\omega\tau) = \frac{d\Phi}{dE} E_1 \quad (18)$$

$$r_1 = \frac{\Phi' E_1}{(1 + i\omega\tau)} \quad (19)$$

In the spirit of [13] we are going to relate this small perturbation behaviour to that of the EIF model under low and high frequencies. First we note that for small frequencies  $r_1$  becomes constant therefore we can match it with the constant value of  $r_1$  in the EIF model to get the value of  $\Phi'$ . On the other hand for the EIF model we have an asymptotic expression for the high frequency limit:

$$\hat{r}_E = \frac{E_1 r_0}{\Delta_T i \omega \tau_m} \quad (20)$$

We include a derivation of the expression in the appendix VI B. Matching this result with the expression above in high frequency we are able to find the value for  $\tau_{eff}$ . We find out that the time constant of the Rate Model is related to the membrane time constant in the following way:

$$\tau_{eff} = \tau_m \frac{\Delta_T \Phi'}{E_1} \quad (21)$$

## B. Space Model

In this section we are going to use the rate model above to construct a spatial model which includes interactions between population of networks. In our spatial model the connections between the network -synaptic connections- affect the input of the neuron in a way such that the perturbation is increased by the spatial effects. We can write that as:  $\tilde{E}(x) = E + \alpha \tau I(x)$  where  $I(x)$  represent the spatial interaction of our network.

$$\tau_x \frac{dr_x}{dt} = \Phi(E + \tau \alpha I(x)) - r_x \quad (22)$$

To model the spatial interaction of our network we are going to use a decaying exponential filter with length constant  $\lambda$ :

$$I(x) = \int_{-\infty}^{\infty} K(x, y) r(y) dy \quad (23)$$

$$= \int_{-\infty}^{\infty} \frac{1}{2\lambda} e^{-\frac{|x-y|}{\lambda}} r(y) dy \quad (24)$$

Where  $I(x)$  is a spatial convolution of the firing rate with an exponential filter. In the appendix (VIC) we work out the next differential equation for the spatial term:

$$\lambda^2 \frac{d^2 I(x)}{dx^2} = I(x) - r_x \quad (25)$$

Therefore our complete coupled system is:

$$\tau_x \frac{dr_x}{dt} = \Phi(E + \tau \alpha I(x)) - r_x \quad (26)$$

$$\lambda^2 \frac{d^2 I(x)}{dx^2} = I(x) - r_x \quad (27)$$

### Steady State

We can solve the steady state firing rate of our firing model by solving the equations self-consistently. First we realize that in one hand  $r_1 = \Phi(\tilde{E})$ . On the other hand using the definition of  $\tilde{E}$  we can also write  $r_2 = \frac{\tilde{E} - E}{\tau \alpha}$ . The intersections of the curves represent the fixed points of the network. Therefore our new  $\tilde{E}$  is given by the zeros of the function:

$$\Phi(\tilde{E}) - \frac{\tilde{E} - E}{\tau \alpha} = 0; \quad (28)$$

### Punctual Perturbation

We can calculate how the network reacts to a rectangular perturbation of the form  $E_1(x) = E_1 (u(x + \frac{L}{2}) - u(x - \frac{L}{2}))$ . Where  $L$  is the wide of the perturbation and  $u(x)$  is the Heaviside Function. In order to study how this affects the firing rate we decompose  $r$  in terms of the steady state and the perturbation:

$$r_0 + r_1 = \Phi(E_0 + E_1(x) + \tau \alpha I_0 + \tau \alpha I_1) \quad (29)$$

Using Taylor's expansion over  $E$  we found that we can write the same expression in the following way:

$$r_0 + r_1 = \Phi(E_0 + \tau \alpha I_1) + \Phi'(E_1(x) + \tau \alpha I_1) \quad (30)$$

But  $r_0 = \Phi(E_0 + \tau \alpha I_1)$  so rearranging appropriately we end up with an expression for the size of the perturbation in terms of the perturbation quantities only:

$$r_1 = \Phi'(E_1(x) + \tau \alpha I_1) \quad (31)$$

On the other hand we have ODE for the connectivity term that involves  $r$ . If we use the last expression we can decouple it from  $r$  and then solve it to obtain  $I_1$  as function of  $x$ . Finally with that expression we can use again the expression above to obtain the spatial profile of  $r_1$ . Proceeding towards that direction and rearranging we have:

$$\lambda^2 \frac{d^2 I_1}{dx^2} = I_1 - \Phi'(E_1(x) + \tau \alpha I_1) \quad (32)$$

$$= I_1 (1 - \Phi' \tau \alpha) - \Phi' E_1(x) \quad (33)$$

$$\frac{\lambda^2}{(1 - \Phi' \tau \alpha)} \frac{d^2 I_1}{dx^2} = I_1 - \frac{\Phi'}{(1 - \Phi' \tau \alpha)} E_1(x) \quad (34)$$



This particular shape in the expression above suggest modified length constant:

$$\lambda_{eff}^2 = \frac{\lambda^2}{(1 - \Phi'\tau\alpha)} \quad (35)$$

Solving this equation and using the appropriate conditions and limits as showed in the appendix VID the solution for  $I$  can be written as follows:

$$I(x) = \frac{E_1\Phi'}{(1 - \Phi'\tau\alpha) \left( \frac{2\lambda_{eff}}{L} + 1 \right)} e^{\frac{-|x|}{\lambda_{eff}}} \quad (36)$$

Then using this equation in conjunction with equation 31 we can finally write the perturbation of the spatial profile:

$$r_1(x) = \frac{E_1\tau\alpha\Phi'^2}{(1 - \Phi'\tau\alpha) \left( \frac{2\lambda_{eff}}{L} + 1 \right)} e^{\frac{-|x|}{\lambda_{eff}}} \quad (37)$$

## V. DISCUSSION AND FURTHER WORK

### A. Discussion

The aim of this research was to study the links between **Spiking Models** and **Network Models**. In order to achieve such a goal the first step was to properly model the spiking neuron models and understand their dynamics. In the first and second sections of the world we have build and studied the appropriated machinery to achieve such a task. We have studied systematically how the rate responds to time dependent and periodic perturbations under two different regimes of noise.

Moreover if we calculate how the perturbations in the rate  $r_1$  depended on the size of the perturbation in  $E$  as in equation 19 and analyse this in conjunction with the frequency dependent dynamic of the perturbation for the EIF system we realize that they can be coupled by their asymptotic behaviour. With this steep we are able to link the parameters of the Firing Rate Model to those of the Spiking Model that comes from faster temporal scale.

Finally with the link provided we can use the Firing Rate model to construct an spatially connected network as in equations 27 and study its response to different spatial perturbations. In particular in this work we have developed the theory to obtain the response to rectangular perturbations 37.

So in conclusion this work has provided a gap between to different models of neuroscience that pertain to different time scales.

### B. Further Work

On the interesting avenues of future work is to study the consequences of the effective length constant in equa-

tion 35  $\lambda_{eff} = \frac{\lambda}{\sqrt{1 - \Phi'\tau\alpha}}$ . In this model when the quantity  $\Phi'\tau\alpha$  comes close to one the length of the effective length constant increases without bound. Close to this conditions the effect of one spike or action potential in a particular region for the network propagates farther and farther as this quantity becomes close to one. In this scenario all the neurons will be strongly interacting and we would like the possible implications and scenarios of such a regime. Further work should go deeper on that particular point.

Furthermore the current state of our system allow us to easily adapt it to study that we can computationally study different spatial perturbation and study the spatio-temporal patterns that result from such scenario.

## VI. APPENDIX

### A. High Frequency Limit for the EIF

From [12] we have:

$$\hat{r}_\alpha = \frac{1}{i} \lim_{s \rightarrow 0} \int_0^\infty dm e^{-(i+s)m} F_\alpha(m) \quad (38)$$

### B. E High Frequency Limit for EIF

For E modulation  $F_E(m) = -m \frac{E_1 r_0}{\Delta_T \omega \tau_0}$  Therefore we have to evaluate the next quantity:

$$\hat{r}_E = \frac{1}{i} \lim_{s \rightarrow 0} \int_0^\infty dm e^{-(i+s)m} - m \frac{E_1 r_0}{\Delta_T \omega \tau_0} \quad (39)$$

$$\hat{r}_E = \frac{E_1 r_0}{\Delta_T \omega \tau_0} \frac{1}{i} \lim_{s \rightarrow 0} \int_0^\infty dm e^{-(i+s)m} - m \quad (40)$$

Our aim is to calculate the integral on the RHS by parts.

$$\int_0^\infty dm e^{-(i+s)m} - m = \frac{m}{i+s} e^{-(i+s)m} \Big|_0^\infty - \frac{1}{i+s} \int_0^\infty dm e^{-(i+s)m} \quad (41)$$

$$\int_0^\infty dm e^{-(i+s)m} - m = \frac{1}{(i+s)^2} e^{-(i+s)m} \Big|_0^\infty \quad (42)$$

$$\int_0^\infty dm e^{-(i+s)m} - m = -\frac{1}{(i+s)^2} \quad (43)$$

From the expression above it follows that:

$$\hat{r}_E = \frac{E_1 r_0}{\Delta_T \omega \tau_0} \frac{1}{i} \lim_{s \rightarrow 0} -\frac{1}{(i+s)^2} \quad (44)$$

$$\hat{r}_E = -\frac{E_1 r_0}{\Delta_T \omega \tau_0} \frac{1}{i^3} \quad (45)$$

$$\hat{r}_E = \frac{E_1 r_0}{i \Delta_T \omega \tau_0} \quad (46)$$

Which is the desired result.

### C. Equation for the spatial term

To derive a differential equation for  $I$  we proceed as follows. The idea is that  $K(x, y) = \frac{1}{2\lambda} e^{-\frac{|x-y|}{\lambda}}$  looks like a Green Function for a differential equation with driving term  $r$ , that is  $\mathcal{L}I = r$ . So if we find a differential equation for the Kernel of the form  $\mathcal{L}K(x, y) = \delta(x - y)$  we will have the desired relation. In order to achieve that end we will use Fourier transform in  $K(x, y)$  as follows:

First we define  $f(x) = e^{-\frac{|x|}{\lambda}}$  therefore we can write  $K(x, y) = \frac{1}{2\lambda} f(x - y)$ . A decaying exponential is a standard function which Fourier's transform is available at tables:  $\mathcal{F}\{f(x)\} = \sqrt{\frac{2}{\pi}} \frac{\frac{1}{\lambda}}{\frac{1}{\lambda^2} + k^2} = \sqrt{\frac{2}{\pi}} \frac{\lambda}{1 + \lambda^2 k^2}$ .

Moreover another standard result from Fourier's transforms theory holds for translations:  $\mathcal{F}\{f(x - y)\} = e^{-iky} \mathcal{F}\{f(x)\}$ . Taking this facts into account we end up with:

$$\mathcal{F}\{K(x, y)\} = \frac{1}{2\lambda} \mathcal{F}\{f(x - y)\} \quad (47)$$

$$= e^{-iky} \frac{1}{\sqrt{2\pi}} \frac{1}{1 + k^2 \lambda^2} \quad (48)$$

Noting that  $-i^2 = 1$  we can write:

$$\mathcal{F}\{K(x, y)\} - \lambda^2 (ik)^2 \mathcal{F}\{K(x, y)\} = e^{-iky} \frac{1}{\sqrt{2\pi}} \quad (49)$$

From Fourier's transforms analysis we also have a relation for the derivative  $\mathcal{F}\{\frac{d^2 f}{dx^2}\} = (ik)^2 \mathcal{F}\{f\}$ . And finally Fourier's theory provides the next frequency representation for the delta function  $\mathcal{F}\{\delta(x)\} = \frac{1}{\sqrt{2\pi}}$ . Using all of the above facts we can made the proceeding rearrangements:

$$\mathcal{F}\{K(x, y)\} - \lambda^2 \mathcal{F}\{\frac{d^2 K(x, y)}{dx^2}\} = e^{-iky} \mathcal{F}\{\delta(x)\} \quad (50)$$

$$\mathcal{F}\{K(x, y) - \lambda^2 \frac{d^2 K(x, y)}{dx^2}\} = \mathcal{F}\{\delta(x - y)\} \quad (51)$$

Using the inverse of the transformation:

$$K(x, y) - \lambda^2 \frac{d^2 K(x, y)}{dx^2} = \delta(x - y) \quad (52)$$

Then our result for  $I(x)$  is:

$$\lambda^2 \frac{d^2 I(x)}{dx^2} = I(x) - r_x \quad (53)$$

### D. Coefficient of the spatial solution

We present here the solution of the next equation:

$$\lambda_{eff}^2 \frac{d^2 I_1}{dx^2} = I_1 - \beta E_1(x) \quad (54)$$

Where  $\beta = \frac{\Phi'}{(1 - \Phi' \tau \alpha)}$  and  $E_1(x)$  is a square pulse which can be written:  $E_1(x) = E_1(u(x + \frac{L}{2}) - u(x - \frac{L}{2}))$ .

Far from the origin the solution to the equation above can be written as:

$$\lambda_{eff}^2 \frac{d^2 I_1}{dx^2} = I_1 \quad (55)$$

Which has exponential solutions. On the other hand far from the origin also the boundary conditions are that  $I_1 = 0$ . That is, we expect the effects of the perturbation to fade away from the perturbation so we can write our solution in the following form:

$$I_1 = A e^{-\frac{|x|}{\lambda_{eff}}} \quad (56)$$

So we need to find  $A$  to completely characterise the function. In order to do so we are going to integrate around the pulse so we have:

$$\lambda_{eff}^2 \frac{dI_1}{dx} \Big|_{-L/2}^{L/2} = AL - \beta E_1 L \quad (57)$$

From the shape of the solution of  $I_1$  we can calculate  $\frac{dI_1}{dx} = -\frac{2A}{\lambda_{eff}}$ . Then using this in the last equation we end up with:

$$A = \frac{E_1 L \beta}{2\lambda_{eff} + L} \quad (58)$$

$$= \frac{\Phi' E_1}{(\frac{2\lambda_{eff}}{L} + 1)(1 - \Phi' \tau \alpha)} \quad (59)$$

### ACKNOWLEDGEMENTS

I am indebted with Erasmus Mundus master program which supported this project financially. I would also like to thanks to Magnus Richardson for his role as a mentor this project.

- 
- [1] E. R. Kandel, J. H. Schwartz, T. M. Jessell, *et al.*, *Principles of neural science*, Vol. 4 (McGraw-Hill New York, 2000).
  - [2] B. Hille, “Ion channels of excitable membranes (sinauer, sunderland, ma),” (2001).
  - [3] E. D. Adrian, *The Journal of physiology* **61**, 49 (1926).
  - [4] F. Rieke, *Spikes: exploring the neural code* (The MIT Press, 1999).
  - [5] W. Gerstner and W. M. Kistler, *Spiking neuron models: Single neurons, populations, plasticity* (Cambridge university press, 2002).
  - [6] P. Dayan, L. F. Abbott, and L. Abbott, *Theoretical neuroscience: Computational and mathematical modeling of neural systems* (MIT press Cambridge, MA, 2001).
  - [7] C. Koch, *Biophysics of Computation: Information Processing in Single Neurons: Information Processing in Single Neurons* (Oxford University Press, USA, 2004).
  - [8] A. L. Hodgkin and A. F. Huxley, *The Journal of physiology* **117**, 500 (1952).
  - [9] L. Lapique, *J. Physiol. Pathol. Gen* **9**, 620 (1907).
  - [10] A. Burkitt, *Biological cybernetics* **95**, 1 (2006).
  - [11] N. Fourcaud-Trocmé, D. Hansel, C. Van Vreeswijk, and N. Brunel, *The Journal of neuroscience* **23**, 11628 (2003).
  - [12] M. J. Richardson, *Physical Review E* **76**, 021919 (2007).
  - [13] S. Ostojic and N. Brunel, *PLoS computational biology* **7**, e1001056 (2011).